Journal of Enzyme Inhibition and Medicinal Chemistry

http://informahealthcare.com/enz
ISSN: 1475-6366 (print), 1475-6374 (electronic)

J Enzyme Inhib Med Chem, 2014; 29(2): 249–255
 DOI: 10.3109/14756366.2013.773994

informa healthcare

ORIGINAL ARTICLE

Synthesis and evaluation of ^{18}F-labeled carbonic anhydrase IX inhibitors for imaging with positron emission tomography

Jinhe Pan[1], Joseph Lau[1], Felix Mesak[1], Navjit Hundal[1], Maral Pourghiasian[1], Zhibo Liu[2], François Bénard[1], Shoukat Dedhar[3], Claudiu T. Supuran[4], and Kuo-Shyan Lin[1]

[1]*Department of Molecular Oncology, BC Cancer Agency, Vancouver, BC, Canada,* [2]*Department of Chemistry, University of British Columbia, Vancouver, BC, Canada,* [3]*Department of Integrative Oncology, BC Cancer Agency, Vancouver, BC, Canada, and* [4]*Polo Scientifico, Laboratorio di Chimica Bioinorganica, Università degli Studi di Firenze, Sesto Fiorentino, Florence, Italy*

Abstract

Two carbonic anhydrase IX (CA IX) inhibitors were radiolabeled with ^{18}F, and evaluated for imaging CA IX expression. Despite good affinity for CA IX and excellent plasma stability, uptake of both tracers in CA IX-expressing HT-29 tumor xenografts in mice was low. ^{18}F-FEC accumulated predominately in the liver and nasal cavity, whereas a significant amount of ^{18}F-U-104 was retained in blood. Due to minimal uptake in HT-29 tumors compared to other organs/tissues, these two tracers are not suitable for use for CA IX-targeted imaging.

Keywords

Benzenesulfonamide, coumarin, cytochrome P450

History

Received 22 January 2013
Accepted 4 February 2013
Published online 7 March 2013

Introduction

Carbonic anhydrase IX (CA IX) is a trans-membrane protein that catalyzes the hydration of carbon dioxide ($CO_2 + H_2O \leftrightarrow H^+ + HCO_3^-$)[1]. CA IX is not expressed in most normal tissues[2] but is highly up-regulated in a variety of solid tumors including bladder[3], cervical[4], head and neck[5], breast[6,7], lung[8] and kidney[9] cancers. The expression of CA IX is induced by the transcription factor HIF-1α, which is stabilized and activated in response to hypoxia[10]. In clear cell renal cell carcinoma (CCRCC) the VHL gene is often mutated, leading to constitutive HIF-1α activation and a strong up-regulation of CA IX expression[11,12]. CA IX expression is associated with poor prognosis and tumor progression[13–15]. CA IX helps cancer cells survive under hypoxia by transporting HCO_3^- into the cell to maintain a neutral intracellular pH[16]. The remaining H^+ acidifies the extracellular microenvironment, activates metalloproteinases and facilitates invasion and metastasis[17–20].

Due to its expression on the cell surface, CA IX is an attractive and accessible target for cancer therapy. There are currently three categories of anti-CA IX therapeutic agents under various stages of clinical trials: (1) sulfonamide derivative Indisulam (E7070) for the treatment of solid tumors[21,22]; (2) the humanized anti-CA IX monoclonal antibody WX-G250 (Rencarex®)[23,24] and (3) anti-CA IX monoclonal antibodies (cG250) radiolabeled with cytotoxic radionuclides (^{131}I and ^{177}Lu) for the treatment of CCRCC[25]. With promising therapeutic agents available, a suitable CA IX-targeted imaging agent is needed to quantify the expression of CA IX in tumors. This will help identify potential responders to CA IX-targeted therapies, and monitor the treatment efficacy. Since CA IX expression in most tumors is generally correlated with hypoxia, CA IX-targeted imaging agents could also be used as a noninvasive imaging tool to visualize hypoxic regions in tumors, and select patients for hypoxia-targeted treatment.

Since its development in the mid-1980s[2], anti-CA IX monoclonal antibody G250 and derivatives have been labeled with ^{131}I, ^{111}In, ^{124}I and ^{89}Zr to image CA IX expression in tumors with single photon emission computed tomography[26,27] or positron emission tomography (PET)[28,29]. Divgi et al.[28] reported that CCRCC could be distinguished accurately from other renal masses by ^{124}I-cG250 PET (94% sensitivity, 100% specificity), supporting the potential clinical use of ^{124}I-cG250 PET in renal masses as an alternative to biopsy for characterizing such lesions. However, the application of radiolabeled anti-CA IX antibodies for imaging hypoxia-associated CA IX expression is limited as the hypoxic tumor regions are usually less accessible to antibodies due to low perfusion caused by aberrant vasculature and increased interstitial pressure. Radiolabeled CA IX-targeted probes derived from small molecule inhibitors will be more suitable because of their ability to diffuse more freely in hypoxic tumor regions. Small molecules are also less expensive to prepare and easier to handle than antibodies, and are not immunogenic.

A large number of small molecule CA IX inhibitors have been developed and several attempts have been made to radiolabel them for imaging. Apte et al.[30] reported the synthesis of an ^{18}F-labeled sulfonamide derivative (Figure 1A), but no biological data were presented. The preparation of a ^{99m}Tc-labeled sulfonamide conjugate (Figure 1B) was reported by Akurathi et al.[31]. Its accumulation in CA IX-expressing HT-29 tumors in mice was minimal with only 0.1% ID/g at 0.5 h post-injection (p.i.). Asakawa et al.[32] reported the radiosynthesis of three potent ^{11}C-ureido-substituted benzenesulfonamides (Figure 1C) as PET

Address for correspondence: Kuo-Shyan Lin, PhD, 675 West 10th Avenue, Rm 4-123, Vancouver, BC V5Z1L3, Canada. Tel: 1-604-675-8208. Fax: 1-604-675-8218. E-mail: klin@bccrc.ca

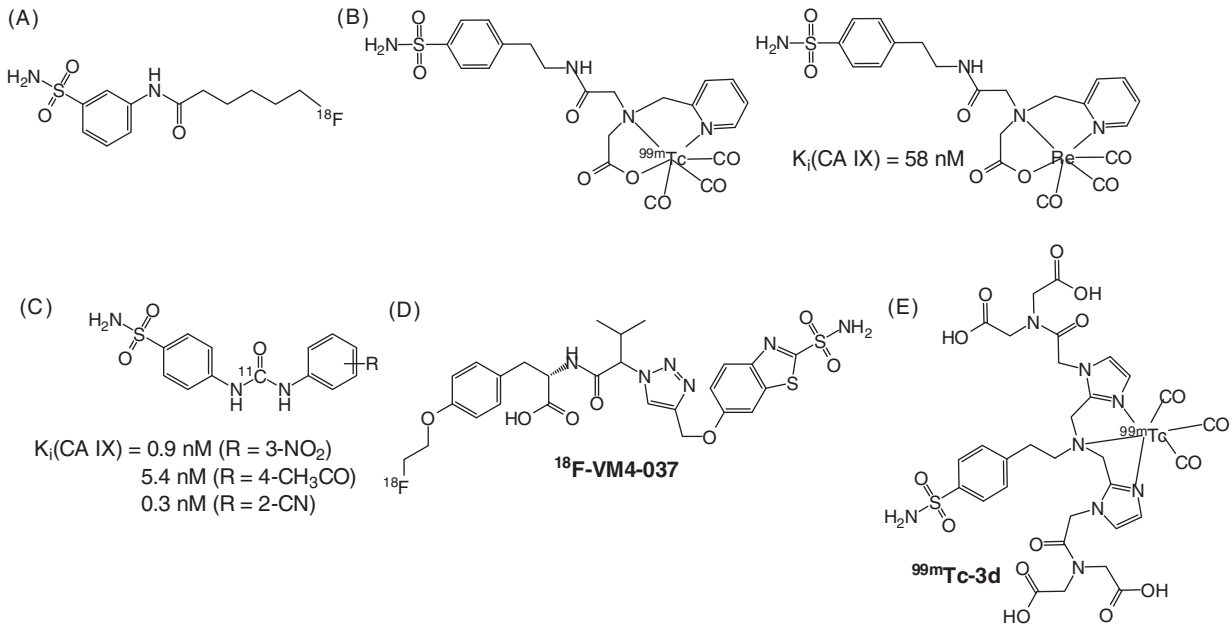

Figure 1. Radiolabeled sulfonamide derivatives for imaging CA IX expression.

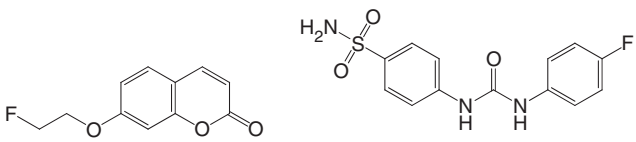

Figure 2. Structures of two potential CA IX inhibitors amenable for radiolabeling with ^{18}F for PET imaging.

probes for imaging CA IX in tumors, but no biological evaluation data were presented. ^{18}F-VM4-037 (Figure 1D), developed by Siemens[33], showed intense background activity in a human study[34], which precluded its use as a cancer imaging agent. Recently, Lu et al. reported the synthesis of a series of ^{99m}Tc/Re-labeled benzenesulfonamide derivative[35]. Among them, ^{99m}Tc-3d (Figure 1E) exhibited high binding affinity ($IC_{50} = 9$ nM) to hypoxic CA IX-expressing HeLa cells, but no further evaluation in animal imaging study was presented. Here, we report our attempts on the synthesis, ^{18}F labeling, and evaluation of two CA IX inhibitors, 7-(2-fluoroethoxy)coumarin (FEC) and U-104 (Figure 2), as potential tracers for imaging CA IX expression with PET.

Materials and methods

Chemicals and instrumentation

U-104[36] and its radiolabeling precursor 4-nitrophenyl 4-sulfamoylcarbanilate[37] were prepared according to previously published procedures. All other chemicals and solvents were obtained from commercial sources, and used without further purification. Proton NMR spectra were obtained using a Bruker (Billerica, MA) Avance 400inv Spectrometer, and were reported in parts per million downfield from internal tetramethylsilane. Mass analyses were performed using a Bruker Esquire-LC/MS system with ESI ion source. Purification and quality control of ^{18}F-labeled CA IX inhibitors were performed on an Agilent (Santa Clara, CA) HPLC System equipped with a model 1200 quaternary pump, a model 1200 UV absorbance detector and a Bioscan (Washington, DC) NaI scintillation detector. The radio-detector was connected to a Bioscan B-FC-1000 Flow-count System, and the output from the Bioscan Flow-count system was fed into an Agilent 35900E Interface which converted the analog signal to digital signal. The operation of the Agilent HPLC system was controlled using the Agilent ChemStation software. The HPLC columns used were a semipreparative column (Phenomenex C18, 5 μ, 250 × 10 mm) and an analytical column (Eclipse XOB-C18, 5 μ, 150 × 4 mm). ^{18}F-Fluoride was produced by the ^{18}O(p, n)^{18}F reaction using an Advanced Cyclotron Systems Inc. (Richmond, BC, Canada) TR19 cyclotron. Radioactivity of ^{18}F-labeled tracers were measured using a Capintec (Ramsey, NJ) CRC®-25R/W dose calibrator, and the radioactivity of mouse tissues collected from biodistribution studies were counted using a Packard (Meriden, CT) Cobra II 5000 Series auto-gamma counter. PET imaging experiments were conducted using a Siemens (Erlangen, Germany) Inveon microPET/CT scanner.

Synthesis of FEC

A mixture of 7-hydroxycoumarin (0.81 g, 5 mmol), 1-fluoro-2-tosyloxyethane (1.56 g, 7.1 mmol) and K_2CO_3 (3.45 g, 25 mmol) in DMF (15 mL) was heated at 70 °C for 24 h. After cooling to room temperature, CH_2Cl_2 (100 mL) was added to the mixture, and the resulted solution was washed with water (100 mL × 3). The CH_2Cl_2 phase was dried with anhydrous $MgSO_4$, concentrated under reduced pressure, and purified by flash column chromatography on silica gel using 4:6 EtOAc/hexanes to obtain the desired product FEC as a white solid (0.918 g, 84 %). ^{1}H NMR ($CDCl_3$) δ 4.28 (dt, $J = 27.6$, 4.0 Hz, 2H), 4.80 (dt, $J = 47.2$, 4.0 Hz, 2H), 6.27 (d, $J = 9.2$ Hz, 1H), 6.83 (d, $J = 2.4$ Hz, 1H), 6.89 (dd, $J = 8.4$, 2.4 Hz, 1H), 7.40 (d, $J = 8.4$ Hz, 1H), 7.65 (d, $J = 9.2$ Hz, 1H); MS (ESI) calculated for $C_{11}H_9FO_3$ $(M + H)^+$ 209.1, found 209.0.

Synthesis of 7-(2-tosyloxyethoxy)coumarin

A solution of 7-hydroxycoumarin (0.81 g, 5 mmol), 1,2-bis(tosyloxy)ethane (2.78 g, 7.5 mmol) and K_2CO_3 (3.45 g, 25 mmol) in DMF (15 mL) was heated at 70 °C for 18 h. After cooling to room temperature, CH_2Cl_2 (100 mL) was added, and the resulted solution was washed with water (100 mL × 3). The CH_2Cl_2 layer was dried with anhydrous $MgSO_4$, concentrated

under reduced pressure, and chromatographed on silica gel using 1:99 CH_3CN/CH_2Cl_2 to obtain the desired product as a white solid (0.282 g, 16%). ^{1}H NMR ($CDCl_3$) δ 2.47 (s, 3H), 4.19–4.25 (m, 2H), 4.39–4.45 (m, 2H), 6.28 (d, $J = 9.2$ Hz, 1H), 6.68 (d, $J = 2.4$ Hz, 1H), 6.76 (dd, $J = 8.4$, 2.4 Hz, 1H), 7.34–7.39 (m, 3H), 7.64 (d, $J = 9.2$ Hz, 1H), 7.83 (d, $J = 8.4$ Hz, 1H); MS (ESI) calculated for $C_{18}H_{16}O_6S$ $(M + H)^+$ 361.1, found 361.1.

Affinity measurement

The inhibition constants (K_i) of FEC to four human CA isoenzymes I, II, IX and XII were determined by CA catalyzed CO_2 hydration assays following previously published procedures[38].

Radiosynthesis of ^{18}F-FEC

The proton-bombarded $H_2[^{18}O]O$ was transferred via He gas push from the cyclotron target station to a Waters (Milford, MA) QMA light Sep-Pak cartridge set up in the hot cell. The ^{18}F-fluoride was trapped in the QMA cartridge, and eluted out into a 4-mL V-shaped reaction vial with a mixture of water (0.3 mL) and CH_3CN (0.3 mL) containing 7 mg of K_2CO_3 and 22 mg of kryptofix 222 (K_{222}). The uncapped reaction vial was placed in a heating block, and the solution was heated at 120 °C. After most of the solvents evaporated, CH_3CN (1 mL × 2) was added to the reaction vial to facilitate complete removal of water. A solution of 7-(2-tosyloxyethoxy)coumarin (3 mg) in DMF (0.5 mL) was added to the reaction vial containing dry $K[^{18}F]F/K_{222}$. The vial was capped, and the mixture was heated at 70 °C for 30 min. At the end of heating, the mixture was diluted with water (1 mL) and purified by HPLC using the semipreparative column eluted with 35% CH_3CN/65% H_2O at a flow rate of 4.5 mL/min. The retention time of ^{18}F-FEC was 17.4 min. The eluting fraction containing ^{18}F-FEC was collected, diluted with water (50 mL), and trapped on a Waters tC18 light Sep-Pak cartridge. After washing the tC18 light Sep-Pak cartridge with water (10 mL), ^{18}F-FEC was eluted out with ethanol (0.4 mL), and formulated with saline (4 mL) for plasma stability study and μPET/CT imaging study. The quality control was performed by HPLC on the analytical column eluted with 25% MeCN/75% H_2O at a flow rate of 2 mL/min. The retention time of ^{18}F-FEC was 8.5 min. The specific activity of ^{18}F-FEC was measured using the analytical HPLC system. It was calculated by dividing the injected radioactivity in 0.2 mL of final ^{18}F-FEC solution by the mass of FEC in the injected solution. The mass of FEC was estimated by comparing the UV absorbance obtained from the injection with a previously prepared standard curve.

Radiosynthesis of ^{18}F-U-104

(1) Radiosynthesis of 1-[^{18}F]fluoro-4-nitrobenzene: a solution of 1,4-dinitrobenzene (4 mg) in DMSO (0.5 mL) was added to a 4 mL reaction vial containing dry $K[^{18}F]F/K_{222}$. The vial was capped, and the mixture was heated at 125 °C for 10 min. At the end of the heating, the mixture was diluted with water (10 mL). The resulted solution was passed through a Waters tC18 plus Sep-Pak cartridge, and the cartridge was washed with water (10 mL). The trapped 1-[^{18}F]fluoro-4-nitrobenzene was eluted out of Sep-Pak cartridge with methanol (1.5 mL). (2) Radiosynthesis of 4-[^{18}F]fluoroaniline. The above solution of 1-[^{18}F]fluoro-4-nitrobenzene in methanol was added to a vial containing 10% palladium on carbon (4 mg) and sodium borohydride (10 mg). The resulted mixture was incubated at room temperature for 5 min. The reaction was quenched by adding 0.1 mL of concentrated HCl and diluted with 1 M NaOH (20 mL). The resulted solution was passed through a Lichrolut EN column (500 mg). The trapped 4-[^{18}F]fluoroaniline in the Lichrolut EN column was eluted out with THF (2 mL) and dried by passing the THF solution through a pre-packed column containing celite (125 mg) and anhydrous $MgSO_4$ (125 mg). (3) Radiosynthesis of ^{18}F-U-104: The above solution of 4-[^{18}F]fluoroaniline in THF was added to a 4-mL reaction vial containing 4-nitrophenyl 4-sulfamoylcarbanilate (8 mg) and DIEA (10 μL) in DMF (0.5 mL). The resulted mixture was heated at 125 °C for 15 min, diluted with water (1 mL), and purified by HPLC using the semipreparative column eluted with 40% MeOH/60% H_2O at a flow rate of 4.5 mL/min. The retention time of ^{18}F-U-104 was 27.4 min. The eluting fraction containing ^{18}F-U-104 was collected, diluted with water (50 mL), and passed through a Waters tC18 light Sep-Pak cartridge. The trapped ^{18}F-U-104 on the Sep-Pak cartridge was eluted out with ethanol (0.4 mL), and formulated with saline (4 mL) for plasma stability and biodistribution studies. The quality control of ^{18}F-U-104 was performed on HPLC using the analytical column eluted with 25% MeCN/75% H_2O at a flow rate of 2 mL/min. The retention time of ^{18}F-U-104 was 7.7 min. The specific activity of ^{18}F-U-104 was measured following same procedures as described for the calculation of specific activity of ^{18}F-FEC.

Stability in mouse plasma

Aliquots (100 μL) of the ^{18}F-labeled tracer (^{18}F-FEC or ^{18}F-U-104) were incubated with 400 μL of balb/c mouse plasma (available from Innovative Research; Cat#: IMS-BCN-N-25 mL) for 5, 15, 30, 60 and 120 min at 37 °C. At the end of each incubation period, samples were passed through a 0.45 micron filter. The filtered sample was loaded onto the analytical HPLC to check the presence of metabolites, and analysis was conducted with Agilent ChemStation software.

In vivo experiments

Mice were maintained and the experiments were conducted in accordance with the guidelines established by the Canadian Council on Animal Care and approved by the Animal Ethics Committee of the University of British Columbia.

Tumor implantation. All experiments were performed using NODSCID IL2RKO mice bred in-house at the Animal Research Centre, British Columbia Cancer Research Centre, Vancouver, Canada. Mice were anesthetized briefly with 2.5% isoflurane in 2.0 L/min of oxygen during cells implantation. After wiping skin surrounding the injection site with an alcohol prep pad, a 31-Gauge needle was used to subcutaneously implant 5×10^6 HT-29 cells (in 100 μL of 1xPBS and BD Matrigel Matrix at 1:1 ratio) under the right shoulder. Biodistribution studies and PET/CT imaging were performed when tumors reached 5–7 mm in diameter.

Biodistribution studies. After HT-29 tumor bearing mice ($n = 3$) were anesthetized using isofluorane, ^{18}F-U-104 was administered intravenously through the caudal vein at a dose of 100 μCi in a volume of 100–200 μL. At 1 h p.i., mice were euthanized by CO_2 asphyxiation followed by cervical dislocation. During dissection, tissues of interest (blood, stomach, intestine, spleen, liver, pancreas, kidney, lung, heart, tumor, muscle, bone and brain) were harvested. Tissues of interest were rinsed with saline (exception of blood), blotted dry, weighed and counted to determine the percentage of injected dose per gram (%ID/g) of tissue.

PET imaging and data analysis. Under anesthesia, 100-200 μCi of [^{18}F]FEC was administered intravenously through

the caudal vein into HT-29 tumor bearing mice ($n = 4$). CT scan was performed before a PET dynamic image sequence of 55 min. PET data were acquired in list mode acquisition. At 1 h p.i., mice were euthanized by CO_2 asphyxiation followed by cervical dislocation. The tissues of interest were harvested, weighed, and counted as described in the above *Biodistribution Studies* section. The PET data were reconstructed using the 3d-OSEM-MAP algorithm with CT-based attenuation correction. Three-dimensional regions of interest were placed on the reconstructed images to determine the %ID/g of tissue using the Inveon Acquisition Workplace software.

Immunohistochemistry

For validation of CA IX expression in HT-29 tumors, histologic tissue analysis was performed. Tumors were harvested and fixed in 4% paraformaldehyde in PBS for 48 h at room temperature. After dehydration, tissues were embedded in paraffin and 4 μm sections were mounted onto poly-L-lysine slides. Immunostaining was performed by the Centre of Translational Applied Genomics at the BC Cancer Agency using the Ventana Discovery XT instrument. Slides were incubated with a goat anti-human CA IX antibody (R&D AF2188) for 1 h without heat at a 1:200 dilution in CC1 antigen retrieval buffer. A rabbit anti-goat linker (1:500) was applied for 32 min followed by a 16 min incubation with Ultramap anti-rabbit HRP detection kit. The stained sections were examined and photographed with a Leica EC3 microscope.

Results and discussion

FEC is a coumarin derivative, whereas U-104 is an ureido-substituted benzenesulfonamide (Figure 2). Both coumarins[39] and benzenesulfonamides[36] have been shown to be potent inhibitors of CA IX. In addition, U-104 has been previously reported to inhibit tumor growth and metastasis in spontaneous and experimental models of metastasis, without inhibitory effects on CA IX-negative tumors[13]. As shown in Scheme 1(A), FEC was synthesized in 84% yield by coupling 7-hydroxycoumarin with 1-fluoro-2-tosyloxyethane[40].

For the development of CA IX-targeted tracers, one concern is the binding to other major CA isoforms including I, II and XII. Cytosolic CA I and CA II are expressed in red blood cells[41,42] and the binding of CA IX-targeted radiotracers to CA I and CA II would increase background signal and reduce the image contrast. On the contrary, binding of these CA IX-targeted radiotracers to CA XII could be beneficial as CA XII is expressed on membranes and is also up-regulated in hypoxic tumors[43]. The inhibition constants (K_i) for human CA isoenzymes I, II, IX and XII were 4622, >100 000, 70, and 88 nM for FEC, respectively. The K_i values for U-104 have been previously reported to be 5080, 95, 45 and 4.5 nM for CA isoenzymes I, II, IX and XII, respectively[13,36].

The radiosynthesis of ^{18}F-FEC was prepared via the ^{18}F aliphatic nucleophilic substitution (Scheme 2A). The radiolabeling precursor, 7-(2-tosyloxyethoxy)coumarin, was prepared by coupling 7-hydroxycoumarin with 1,2-bis(tosyloxy)ethane in 16% yield (Scheme 1B). After HPLC purification, ^{18}F-FEC was obtained in 11–24 % decay-corrected yield in 1.6 h synthesis time with 1.7–5.7 Ci/μmol specific activity at the end of synthesis (EOS), and >99% radiochemistry purity. The preparation of ^{18}F-U-104 was depicted in Scheme 2(B). The radiosynthesis involves three reactions. First, 1-[^{18}F]fluoro-4-nitrobenzene was prepared in 40–60% radiochemical yield by direct aromatic nucleophilic substitution reaction using ^{18}F-fluoride and dinitrobenzene. The isolated 1-[^{18}F]fluoro-4-nitrobenzene was reduced to 4-[^{18}F]fluoroaniline in >90 % yield following previously published procedure[44] using $NaBH_4$ and 10% Pd/C. At the final step, ^{18}F-U-104 was obtained in >50% radiochemical yield by reacting 4-[^{18}F]fluoroaniline with 4-nitrophenyl 4-sulfamoylcarbanilate in DMF. However, due to multiple purification steps, ^{18}8F-U-104 isolated in only 3–9% overall decay-corrected yield in 2.5 h synthesis time with >98% radiochemical purity, and 15.1–19.8 Ci/μmol specific activity at EOS. The reason that ^{18}F-U-104 had much higher specific activity than ^{18}F-FEC was because we used Teflon tubing as the H[^{18}F]F/H_2[^{18}O]O transfer line

Scheme 1. Synthesis of (A) FEC and (B) its radiolabeling precursor 7-(2-tosyloxyethoxy)coumarin.

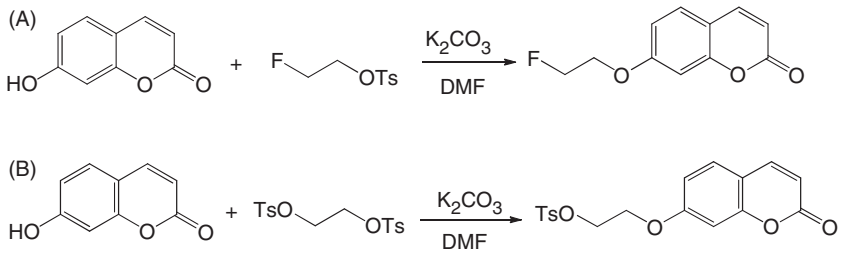

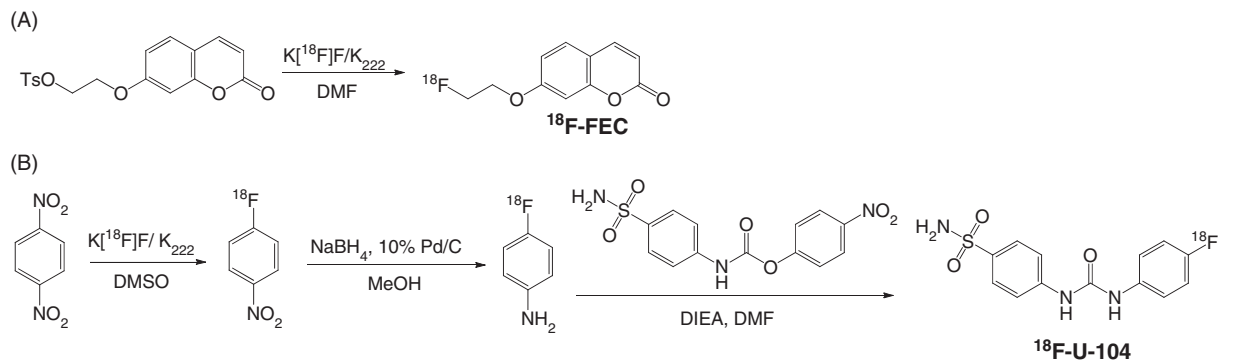

Scheme 2. Radiosynthesis of (A) ^{18}F-FEC and (B) ^{18}F-U-104.

while preparing ^{18}F-FEC. Before working on ^{18}F-U-104, we replaced the Teflon transfer line with peek tubing. This change reduced the amount of fluoride leaching out from the transfer line, and significantly increased the specific activities of ^{18}F-labeled tracers including ^{18}F-U-104 prepared thereafter.

Both ^{18}F-U-104 and ^{18}F-FEC were stable in mouse plasma with >99% of the tracers remaining intact after 2 h incubation at 37 °C. For the imaging/biodistribution studies, we used HT-29 colorectal tumor xenografts as our CA IX-expressing tumor model, and the expression of CA IX in the tumors was confirmed by immunohistochemistry (Figure 3). Due to its constitutive expression of CA IX, HT-29 cells have also been used by other investigators[31,45] as a CA IX-expressing model for the development of CA IX-targeted tracers.

The biodistribution data of ^{18}F-U-104 (Table 1) indicated that the radioactivity was excreted via both renal and hepatobiliary pathways. The uptake in intestines and kidneys at 1 h p.i. were 13.66 ± 1.23 and 9.71 ± 1.68 %ID/g, respectively. Tumor uptake (%ID/g) of ^{18}F-U-104 at 1 h p.i. was 0.83 ± 0.06 which was lower than blood (13.92 ± 3.07), muscle (1.19 ± 0.20) and major organs except brain (0.16 ± 0.01). High blood uptake of ^{18}F-U-104 is likely due to the binding to CA II in erythrocytes. U-104 has good affinity (95 nM) for CA II and it has been shown that erythrocytes express high level of CA II[41,42]. Due to minimal uptake of ^{18}F-U-104 in HT-29 tumors compared to normal tissues/organs, ^{18}F-U-104 is not suitable for use for CA IX-targeted imaging.

Biodistribution and PET imaging studies of ^{18}F-FEC showed that the radioactivity was excreted via both renal and hepatobiliary pathways (Table 1, Figure 4). *In vivo* defluorination of ^{18}F-FEC was likely as uptake in bone (2.09 ± 0.50 %ID/g) was higher than the uptake in both blood (1.54 ± 0.44 %ID/g) and muscle (0.73 ± 0.13 %ID/g) at 1 h p.i. Tumor uptake of ^{18}F-FEC was 1.16 ± 0.19 %ID/g at 1 h p.i. The tumors were not visualized from PET image (Figure 4) due to low tumor uptake and very high liver uptake (33.76 ± 8.31 %ID/g at 1 h p.i.). The high uptake in the liver was not simply due to the hepatobiliary excretion of ^{18}F-FEC as the uptake in intestines was low (3.14 ± 1.24 %ID/g) and the uptake in the liver did not decrease over time (Figure 5).

One possible explanation for the high uptake of ^{18}F-FEC in the liver is due the action of 7-ethoxycoumarin O-deethylase (ECOD). ECOD is a family of cytochrome P450 enzymes that metabolize 7-ethoxycoumarin into 7-hydroxycoumarin and acetaldehyde[46] as depicted in Scheme 3(A). ECOD is highly expressed in the liver, and one of the major ECOD is CYP1A2[46,47]. Due to the similarity of 7-ethoxycoumarin and FEC in their structures, it is likely that ECOD also metabolizes ^{18}F-FEC into 7-hydroxycoumarin and 2-[^{18}F]fluoroacetaldehyde (Scheme 3B). The radioactive metabolite 2-[^{18}F]fluoroacetaldehyde can be further metabolized into 2-[^{18}F]fluoroacetate which in turn forms 2-[^{18}]fluoroacetyl CoA and becomes trapped within the cell[48]. This hypothesis was supported by the high uptake of ^{18}F-FEC observed in the nasal cavity (Figures 4 and 5) as

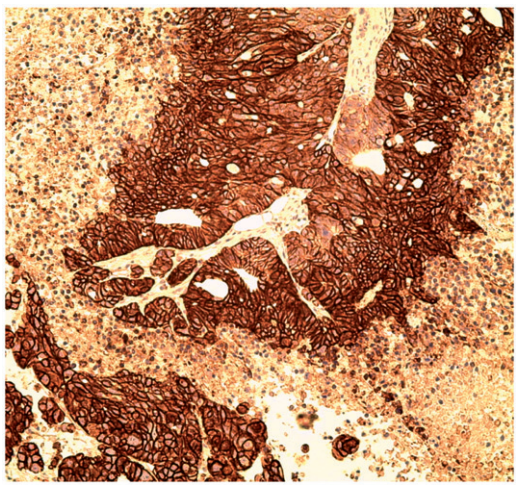

Figure 3. Immunohistochemical staining of CA IX expression in a HT-29 tumor.

Table 1. Biodistribution of ^{18}F-FEC and ^{18}F-U-104 in HT-29 tumor bearing NODSCID IL2RKO mice at 1 h post injection.

	^{18}F-FEC	^{18}F-U-104
Blood	1.54 ± 0.44	13.92 ± 3.07
Stomach	0.89 ± 0.46	2.94 ± 2.28
Intestine	3.14 ± 1.24	13.66 ± 1.23
Spleen	1.89 ± 0.88	6.48 ± 0.74
Liver	33.76 ± 8.31	6.76 ± 0.22
Pancreas	0.77 ± 0.10	3.33 ± 0.11
Kidney	6.97 ± 3.34	9.71 ± 1.68
Lungs	1.18 ± 0.24	5.71 ± 0.42
Heart	1.16 ± 0.27	3.46 ± 0.57
Tumor	1.16 ± 0.19	0.83 ± 0.06
Muscle	0.73 ± 0.13	1.19 ± 0.20
Bone	2.09 ± 0.50	2.52 ± 0.81
Brain	0.88 ± 0.16	0.16 ± 0.01

Data are expressed as %ID/g ± S.D.

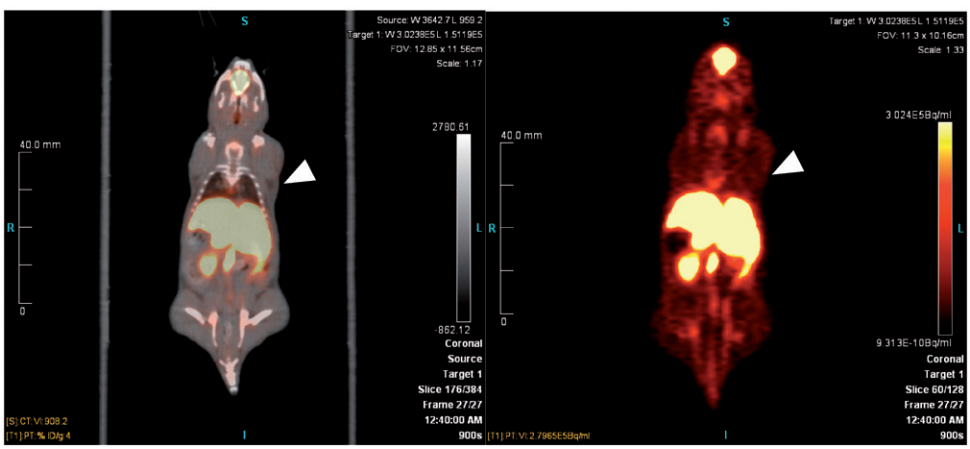

Figure 4. A typical PET image of ^{18}F-FEC in HT-29 tumor bearing NODSCID IL2RKO mice at 55 min post-injection. White arrows indicate tumor.

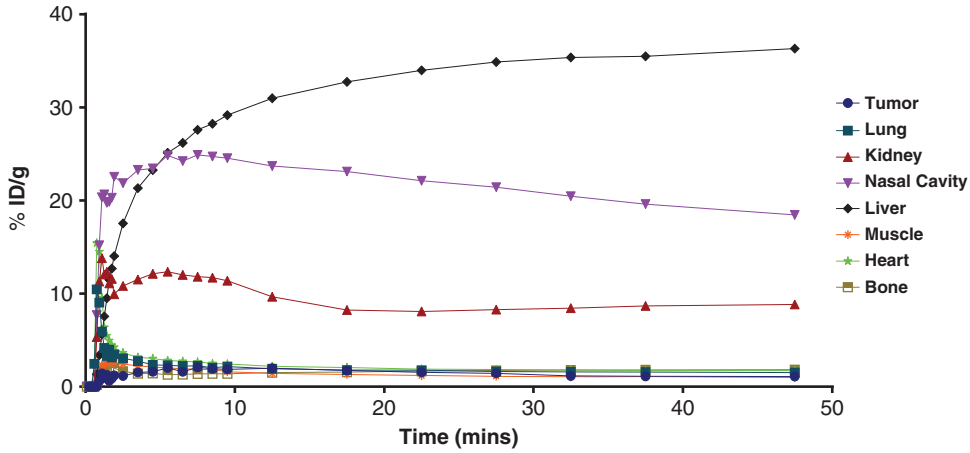

Figure 5. Time-activity curve of ^{18}F-FEC in tumor and selected organs/tissues.

Scheme 3. (A) Metabolism of 7-ethoxycoumarin and (B) proposed metabolism of ^{18}F-FEC by ECOD.

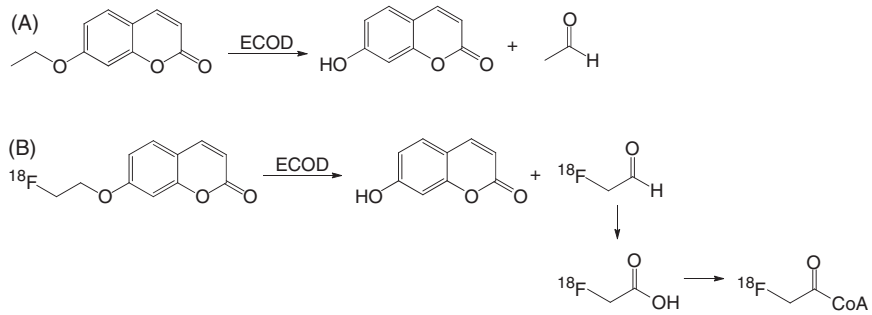

olfactory mucosa is the only extrahepatic tissue expressing high level of CPY1A2[49]. However, more studies are needed to confirm the trapping mechanism of ^{18}F-FEC in the liver and nasal cavity.

Conclusions

We have synthesized two ^{18}F-labeled CA IX inhibitors, ^{18}F-FEC and ^{18}F-U-104, and evaluated their potential as CA IX-targeted PET tracers. Both compounds showed good affinity for CA IX and excellent stability in mouse plasma. However, their uptake in CA IX-expressing HT-29 tumors was minimal which precludes their application as CA IX imaging agents. The unexpected trapping of ^{18}F-FEC in the liver and nasal cavity could be due to the metabolism of ^{18}F-FEC by ECOD. Once this is confirmed, ^{18}F-FEC may be potentially used for imaging the expression/activity of ECOD with PET.

Acknowledgements

We are thankful to Jean-Pierre Appiah and Milan Vuckovic for operating the cyclotron and providing ^{18}F-fluoride for radiolabeling experiments.

Declaration of interest

This work was supported by the Canadian Institutes of Health Research (Grant MOP 102685), and the postdoctoral position held by Jinhe Pan was funded by the Canadian Breast Cancer Foundation. The authors report no declarations of interest.

References

1. Supuran CT. Carbonic anhydrases: novel therapeutic applications for inhibitors and activators. Nat Rev Drug Discov 2008;7:168–81.
2. Oosterwijk E, Ruiter DJ, Hoedemaeker PJ, et al. Monoclonal antibody G-250 recognizes a determinant present in renal-cell carcinoma and absent from normal kidney. Int J Cancer 1986;38:489–94.
3. Ord JJ, Agrawal S, Thamboo TP, et al. An investigation into the prognostic significance of necrosis and hypoxia in high grade and invasive bladder cancer. J Urol 2007;178:677–82.
4. Hutchison GJ, Valentine HR, Loncaster JA, et al. Hypoxia-inducible factor lot expression as an intrinsic marker of hypoxia: Correlation with tumor oxygen, pimonidazole measurements, and outcome in locally advanced carcinoma of the cervix. Clin Cancer Res 2004;10:8405–12.
5. Koukourakis MI, Bentzen SM, Giatromanolaki A, et al. Endogenous markers of two separate, hypoxia response pathways (hypoxia inducible factor 2 alpha and carbonic anhydrase 9) are associated with radiotherapy failure in head and neck cancer patients recruited in the CHART randomized trial. J Clin Oncol 2006;24:727–35.
6. Trastour C, Benizri E, Ettore F, et al. HIF-1 alpha and CA IX staining in invasive breast carcinomas: prognosis and treatment outcome. Int J Cancer 2007;120:1451–8.
7. Hussain SA, Ganesan R, Reynolds G, et al. Hypoxia-regulated carbonic anhydrase IX expression is associated with poor survival in patients with invasive breast cancer. Brit J Cancer 2007;96:104–9.
8. Swinson DEB, Jones JL, Richardson D, et al. Carbonic anhydrase IX expression, a novel surrogate marker of tumor hypoxia, is associated with a poor prognosis in non-small-cell lung cancer. J Clin Oncol 2003;21:473–82.
9. Dorai T, Sawczuk I, Pastorek J, et al. Role of carbonic anhydrases in the progression of renal cell carcinoma subtypes: proposal of a unified hypothesis. Cancer Invest 2006;24:754–79.
10. Wykoff CC, Beasley NJP, Watson PH, et al. Hypoxia-inducible expression of tumor-associated carbonic anhydrases. Cancer Res 2000;60:7075–83.
11. Mandriota SJ, Turner KJ, Davies DR, et al. HIF activation identifies early lesions in VHL kidneys: evidence for site-specific tumor suppressor function in the nephron. Cancer Cell 2002;1:459–68.
12. Ivanov SV, Kuzmin I, Wei MH, et al. Down-regulation of transmembrane carbonic anhydrases in renal cell carcinoma cell lines by wild-type von Hippel-Lindau transgenes. Proc Natl Acad Sci USA 1998;95:12596–601.

13. Lou Y, McDonald PC, Oloumi A, et al. Targeting tumor hypoxia: suppression of breast tumor growth and metastasis by novel carbonic anhydrase IX inhibitors. Cancer Res 2011;71:3364–76.
14. Korkeila E, Talvinen K, Jaakkola PM, et al. Expression of carbonic anhydrase IX suggests poor outcome in rectal cancer. Brit J Cancer 2009;100:874–80.
15. Koukourakis MI, Giatromanolaki A, Sivridis E, et al. Hypoxia-activated tumor pathways of angiogenesis and pH regulation independent of anemia in head-and-neck cancer. Int J Radiat Oncol Biol Phys 2004;59:67–71.
16. Swietach P, Hulikova A, Vaughan-Jones RD, Harris AL. New insights into the physiological role of carbonic anhydrase IX in tumour pH regulation. Oncogene 2010;29:6509–21.
17. Svastova E, Hulikova A, Rafajova M, et al. Hypoxia activates the capacity of tumor-associated carbonic anhydrase IX to acidify extracellular pH. FEBS Lett 2004;577:439–45.
18. Swietach P, Vaughan-Jones RD, Harris AL. Regulation of tumor pH and the role of carbonic anhydrase 9. Cancer Metast Rev 2007;26: 299–310.
19. Kroemer G, Pouyssegur J. Tumor cell metabolism: ancer's achilles' heel. Cancer cell 2008;13:472–82.
20. Stock C, Schwab A. Protons make tumor cells move like clockwork. Pflug Arch Eur J Physiol 2009;458:981–92.
21. Supuran CT. Indisulam: an anticancer sulfonamide in clinical development. Expert Opin Investig Drugs 2003;12:283–7.
22. Thiry A, Dogne JM, Masereel B, Supuran CT. Targeting tumor-associated carbonic anhydrase IX in cancer therapy. Trends Pharmacol Sci 2006;27:566–73.
23. Siebels M, Rohrmann K, Oberneder R, et al. A clinical phase I/II trial with the monoclonal antibody cG250 (RENCAREX®) and interferon-alpha-2a in metastatic renal cell carcinoma patients. World J Urol 2011;29:121–6.
24. Belldegrun A. Chimeric monoclonal antibody cG250 (Rencarex®) as immunotherapy of renal cell carcinoma: clinical Phase II summary and current adjuvant Phase III trial in non-metastasized RCC after nephrectomy. Ann Oncol 2005;16:18.
25. Stillebroer AB, Mulders PFA, Boerman OC, et al. Carbonic anhydrase IX in renal cell carcinoma: implications for prognosis, diagnosis, and therapy. Eur Urol 2010;58:75–83.
26. Brouwers AH, Dorr U, Lang O, et al. ^{131}I-cG250 monoclonal antibody immunoscintigraphy versus [^{18}F]FDG-PET imaging in patients with metastatic renal cell carcinoma: a comparative study. Nucl Med Commun 2002;23:229–36.
27. Brouwers AH, Buijs WC, Boerman OC, et al. Higher uptake in renal cell carcinoma (RCC) metastases with In-111-labeled chimeric monoclonal antibody G250 (cG250) than with I-131-cG250 in an intra-patient comparison. J Nucl Med 2003;44:171P–2P.
28. Divgi CR, Pandit-Taskar N, Jungbluth AA, et al. Preoperative characterisation of clear-cell renal carcinoma using iodine-124-labelled antibody chimeric G250 (^{124}I-cG250) and PET in patients with renal masses: a phase I trial. Lancet Oncol 2007;8:304–10.
29. Hoeben BAW, Kaanders JHAM, Franssen GM, et al. PET of hypoxia with ^{89}Zr-Labeled cG250-F(ab′)$_2$ in head and neck tumors. J Nucl Med 2010;51:1076–83.
30. Apte SD, Chin FT, Graves EE. Synthesis of a new PET radiotracer targeting carbonic anhydrase IX. J Label Compd Radiopharm 2009; 52:S408.
31. Akurathi V, Dubois L, Lieuwes NG, et al. Synthesis and biological evaluation of a ^{99m}Tc-labelled sulfonamide conjugate for in vivo visualization of carbonic anhydrase IX expression in tumor hypoxia. Nucl Med Biol 2010;37:557–64.
32. Asakawa C, Ogawa M, Kumata K, et al. Radiosynthesis of three [^{11}C]ureido-substituted benzenesulfonamides as PET probes for carbonic anhydrase IX in tumors. Bioorg Med Chem Lett 2011;21: 7017–20.
33. Kolb HC, Walsh JC, Kasi D, et al. Development of molecular imaging probes for carbonic anhydrase-IX using click chemistry. US Patent 0317842; 2010.
34. Doss M, Alpaugh RK, Yu JQ. Biodistribution and radiation dosimetry of CA-IX PET imaging agent ^{18}F-VM4-037 measured in healthy volunteers. Mol Imaging Biol 2010;12:S124.
35. Lu G, Hillier SM, Maresca KP, et al. Synthesis and SAR of novel Re/^{99m}Tc-labeled benzenesulfonamide carbonic anhydride IX inhibitors for molecular imaging of tumor hypoxia. J Med Chem 2013;56:510–20.
36. Pacchiano F, Carta F, McDonald PC, et al. Ureido-substituted benzenesulfonamides potently inhibit carbonic anhydrase IX and show antimetastatic activity in a model of breast cancer metastasis. J Med Chem 2011;54:1896–902.
37. Baker BR, Hurlbut JA. Irreversible enzyme inhibitors. CLIIIProteolytic enzymes 11 Inhibition of guinea pig complement by substituted phenoxyacetamides. J Med Chem 1969;12:415–19.
38. Carta F, Maresca A, Scozzafava A, Supuran CT. Novel coumarins and 2-thioxo-coumarins as inhibitors of the tumor-associated carbonic anhydrases IX and XII. Bioorg Med Chem 2012;20: 2266–73.
39. Touisni N, Maresca A, McDonald PC, et al. Glycosyl coumarin carbonic anhydrase IX and XII inhibitors strongly attenuate the growth of primary breast tumors. J Med Chem 2011;54:8271–7.
40. Wilson AA, Dasilva JN, Houle S. Synthesis of two radiofluorinated cocaine analogs using distilled 2-[^{18}F]fluoroethyl bromide. Appl Radiat Isot 1995;46:765–70.
41. Gokce B, Gencer N, Arslan O, et al. Evaluation of *in vitro* effects of some analgesic drugs on erythrocyte and recombinant carbonic anhydrase I and II. J Enzym Inhib Med Chem 2012;27:37–42.
42. Senturk M, Gulcin I, Beydemir S, et al. *In vitro* inhibition of human carbonic anhydrase I and II isozymes with natural phenolic compounds. Chem Biol Drug Des 2011;77:494–9.
43. Guler OO, de Sımone G, Supuran CT. Drug design studies of the novel antitumor targets carbonic anhydrase IX and XII. Curr Med Chem 2010;17:1516–26.
44. Hendricks JA, Keliher EJ, Marinelli B. *In vivo* PET imaging of histone deacetylases by ^{18}F-suberoylanilide hydroxamic acid (^{18}F-SAHA). J Med Chem 2011;54:5576–82.
45. Groves K, Bao B, Zhang J, et al. Synthesis and evaluation of near-infrared fluorescent sulfonamide derivatives for imaging of hypoxia-induced carbonic anhydrase IX expression in tumors. Bioorg Med Chem Lett 2012;22:653–7.
46. Kim KH, Isin EM, Yun CH, et al. Kinetic deuterium isotope effects for 7-alkoxycoumarin O-dealkylation reactions catalyzed by human cytochromes P450 and in liver microsomes – rate-limiting C–H bond breaking in cytochrome P450 1A2 substrate oxidation. FEBS J 2006;273:2223–31.
47. Yamazaki H, Inoue K, Mimura M, et al. 7-ethoxycoumarin O-deethylation catalyzed by cytochromes P450 1A2 and 2E1 in human liver microsomes. Biochem Pharmacol 1996;51:313–19.
48. Tewson TJ, Welch MJ. Preparation and preliminary biodistribution of no carrier added F-18 fluoroethanol. J Nucl Med 1980;21: 559–64.
49. Ling G, Gu J, Genter MB, et al. Regulation of cytochrome P450 gene expression in the olfactory mucosa. Chem Biol Interact 2004; 147:247–58.